Miyake, Y., Shiroyama, N., Ota, I., Horiguchi, M., 1988. Oscillatory potentials in electroretinograms of the human macular region. Invest. Ophthalmol. Vis. Sci. 29, 1631–1635.

Miyake, Y., Shiroyama, N., Horiguchi, M., Ota, I., 1989. Asymmetry of focal ERG in human macular region. Invest. Ophthalmol. Vis. Sci. 30, 1743–1749.

Miyata, K., Nakamura, M., Kondo, M., Lin, J., Ueno, S., Miyake, Y., Terasaki, H., 2007. Reduction of oscillatory potentials and photopic negative response in patients with autosomal dominant optic atrophy with OPA1 mutations. Invest. Ophthalmol. Vis. Sci. 48, 820–824.

Perry, V.H., Cowey, A., 1985. The ganglion cell and cone distributions in the monkey's retina: implications for central magnification factors. Vision Res. 25, 1795–1810.

Porrello, G., Falsini, B., 1999. Retinal ganglion cell dysfunction in humans following post-geniculate lesions: specific spatio-temporal losses revealed by pattern ERG. Vision Res. 39, 1739–1745.

Rangaswamy, N.V., Hood, D.C., Frishman, L.J., 2003. Regional variations in local contributions to the primate photopic flash ERG: revealed using the slow-sequence mfERG. Invest. Ophthalmol. Vis. Sci. 44, 3233–3247.

Rangaswamy, N.V., Frishman, L.J., Dorotheo, E.U., Schiffman, J.S., Bahrani, H.M., Tang, R.A., 2004. Photopic ERGs in patients with optic neuropathies: comparison with primate ERGs after pharmacologic blockade of inner retina. Invest. Ophthalmol. Vis. Sci. 45, 3827–3837.

Rangaswamy, N.V., Shirato, S., Kaneko, M., Digby, B.I., Robson, J.G., Frishman, L.J., 2007. Effects of spectral characteristics of Ganzfeld stimuli on the photopic negative response (PhNR) of the ERG. Invest. Ophthalmol. Vis. Sci. 48, 4818–4828.

Rangaswamy, N.V., Zhou, W., Harwerth, R.S., Frishman, L.J., 2006. Effect of experimental glaucoma in primates on oscillatory potentials of the slow-sequence mfERG. Invest. Ophthalmol. Vis. Sci. 47, 753–767.

Silveira, L.C., Picanço-Diniz, C.W., Sampaio, L.F., Oswaldo-Cruz, E., 1989. Retinal ganglion cell distribution in the cebus monkey: a comparison with the cortical magnification factors. Vision Res. 29, 1471–1483.

Silveira, L.C., Perry, V.H., Yamada, E.S., 1993. The retinal ganglion cell distribution and the representation of the visual field in area 17 of the owl monkey, *Aotus trivirgatus*. Vis. Neurosci. 10, 887–897.

Ueno, S., Kondo, M., Niwa, Y., Terasaki, H., Miyake, Y., 2004. Luminance dependence of neural components that underlies the primate photopic electroretinogram. Invest. Ophthalmol. Vis. Sci. 45, 1033–1040.

Ueno, S., Kondo, M., Ueno, M., Miyata, K., Terasaki, H., Miyake, Y., 2006. Contribution of retinal neurons to d-wave of primate photopic electroretinograms. Vision Res. 46, 658–664.

Viswanathan, S., Frishman, L.J., Robson, J.G., Harwerth, R.S., Smith III, E.L., 1999. The photopic negative response of the macaque electroretinogram: reduction by experimental glaucoma. Invest. Ophthalmol. Vis. Sci. 40, 1124–1136.

Viswanathan, S., Frishman, L.J., Robson, J.G., 2000. The uniform field and pattern ERG in macaques with experimental glaucoma: removal of spiking activity. Invest. Ophthalmol. Vis. Sci. 41, 2797–2810.

Viswanathan, S., Frishman, L.J., Robson, J.G., Walters, J.W., 2001. The photopic negative response of the flash electroretinogram in primary open angle glaucoma. Invest. Ophthalmol. Vis. Sci. 42, 514–522.

Wu, S., Sutter, E.E., 1995. A topographic study of oscillatory potentials in man. Vis. Neurosci. 12, 1013–1025.

Yoshii, M., Päärmann, A., 1989. Hemiretinal stimuli elicit different amplitudes in the pattern electroretinogram. Doc. Ophthalmol. 72, 21–30.

Zhou, W., Rangaswamy, N., Ktonas, P., Frishman, L.J., 2007. Oscillatory potentials of the slow-sequence multifocal ERG in primates extracted using the Matching Pursuit method. Vision Res. 47, 2021–2036.

CONCENTRATION OF VASCULAR ENDOTHELIAL GROWTH FACTOR IN AQUEOUS HUMOR OF EYES WITH ADVANCED RETINOPATHY OF PREMATURITY BEFORE AND AFTER INTRAVITREAL INJECTION OF BEVACIZUMAB

NORIE ITO NONOBE, MD, SHU KACHI, MD, PHD, MINEO KONDO, MD, PHD, YOSHIKO TAKAI, MD, PHD, KOJI TAKEMOTO, MD, ATSUSHI NAKAYAMA, MD, MASAHIRO HAYAKAWA, MD, PHD, HIROKO TERASAKI, MD, PHD

Purpose: To determine whether an intravitreal injection of bevacizumab alters the concentration of vascular endothelial growth factor (VEGF) in the aqueous humor of eyes with retinopathy of prematurity.

Methods: Seven Stage 4 and three Stage 5 eyes of eight patients with retinopathy of prematurity were studied. Bevacizumab (0.75 mg/0.03 mL/eye) was injected intravitreally in six eyes of six patients after approval was obtained from the Institutional Review Board of Nagoya University Hospital and an informed consent was signed by the parents. Aqueous humor was collected just before the surgery or before the intravitreal injection of bevacizumab. Aqueous humor was also collected immediately before vitrectomy 4 to 48 days after the injection of bevacizumab. Aqueous humor was also collected from four patients undergoing congenital cataract surgery as controls. The concentration of VEGF was measured by enzyme-linked immunosorbent assay.

Results: In the 4 control eyes, the concentration of VEGF in 2 eyes was 156 and 158 pg/mL and was not detectable in the other 2 eyes. The average concentration of VEGF was 1,109 pg/mL in the active Stage 4 eyes and 3,520 pg/mL in the active Stage 5 eyes. After bevacizumab injection, the unbound VEGF concentration was 60, 230, and 290 pg/mL in 3 eyes and not detectable in 1 eye.

Conclusion: Intravitreal bevacizumab resulted in a marked decrease in the unbound VEGF concentration in eyes with retinopathy of prematurity.

RETINA 29:579–585, 2009

Vascular endothelial growth factor (VEGF) is a dimeric glycoprotein that plays an important role in angiogenesis and neovascularization.[1] The retina is known to be ischemic in certain ocular diseases, such as diabetic retinopathy and retinopathy of prematurity (ROP), and the expression of VEGF is up-regulated, which leads to retinal neovascularization. This is important because the neovascularization can progress to vitreous hemorrhage, proliferative membranes, and retinal detachments (RDs).[2–4] Thus, one of the strategies to prevent these vision-threatening changes is to block the upregulation of VEGF.

From the Department of Ophthalmology, Nagoya University Graduate School of Medicine, Tsurumai, Showa-ku, Nagoya, Japan.

Grant-in-Aid for Scientific Research from the Ministry of Education, Culture, Sports, Science, and Technology of Japan [19791262 (S.K.), 18390466 (H.T.)].

Reprint requests: Hiroko Terasaki, MD, PhD, Department of Ophthalmology, Nagoya University Graduate School of Medicine, 65 Tsurumai, Showa-ku, Nagoya 466-8550, Japan; e-mail: terasaki@med.nagoya-u.ac.jp

Bevacizumab (Avastin; Genentech Inc., San Francisco, CA) is a humanized anti-VEGF monoclonal antibody that has been used systemically to treat patients with cancer.[5] For the eye, an intravitreal injection of bevacizumab was found to be effective in reducing the severity of ocular diseases such as neovascular age-related macular degeneration,[6] retinal vein occlusion,[7] and diabetic retinopathy.[8] Bevacizumab has also been used as a preoperative adjunctive therapy for proliferative diabetic retinopathy (PDR).[9] Sawada et al[10] have reported a marked decrease of ocular unbound VEGF level after an intravitreal injection of bevacizumab in eyes with PDR suggesting that the effectiveness of bevacizumab was due to a reduction of the unbound VEGF level.

ROP is a major cause of serious visual impairment in infants born prematurely, and the number of cases of severe ROP is increasing with the increase in the survival rate of the smallest pronatis.[11] In most cases, retinal photocoagulation is very effective in treating eyes with ROP, and the photocoagulation leads to a quiescent stage. However, despite this treatment, some eyes progress to the advanced stages of ROP with proliferative membranes and RDs. For severe cases, vitrectomy must be performed to reattach the retina, although surgeons must wait for the neovascular membranes to become quiescent, which greatly hinders the prognosis of good vision.

VEGF plays a key role in progression of ROPs, and Chung et al[12] have reported that bevacizumab was effective in treating eyes with ROP. This finding suggested that preoperative bevacizumab can be an effective adjunctive therapy for ROP. To the best of our knowledge, there have been only two studies on the ocular VEGF level in eyes with ROP,[13,14] and neither of these reported the level of VEGF after an intravitreal injection of bevacizumab.

Thus, the purpose of this study was to measure the concentration of VEGF in the aqueous humor in eyes with Stage 4 and Stage 5 ROP before and after an intravitreal injection of bevacizumab.

Methods

Subjects

Approval for this study was obtained from the Institutional Review Board of Nagoya University Hospital, and an informed consent was obtained from the parents. The procedures used in this study conformed to the tenets of the Declaration of Helsinki.

Seven eyes at Stage 4 and three at Stage 5 of eight patients with ROP were studied (Table 1). The mean postmenstrual age of the patients was 41.1 weeks (35–64 weeks). Bevacizumab at a dosage of 0.75 mg/0.03 mL was injected intravitreally in 6 eyes of 6 patients. An encircling or buckling procedure was performed on four eyes at Stage 4 ROP. Vitrectomy with lensectomy was performed on two Stage 4B and on two Stage 5 ROP eyes after bevacizumab injection, and in one Stage 5 ROP eye without an injection.

Aqueous humor was collected just before the surgery from seven eyes at Stage 4 and three at Stage 5 eyes. Aqueous humor was also collected just before the intravitreal injection of bevacizumab from two eyes at Stage 4 and two at Stage 5. For control, aqueous humor was also collected from three eyes with congenital cataract and one eye with persistent pupillary membrane that underwent surgery (1 male and 3 female infants). The mean age of these patients was 4.0 ± 2.1 months with a range of 2 to 7 months. Ophthalmoscopy showed that the fundus was normal in these four eyes. Although the eyes used as control were younger than that used in a previous report,[14] they were still older than the ROP eyes. This difference in the ages might have altered the VEGF level.

Ophthalmologic Examinations and Staging of Retinopathy of Prematurity

Fundus and 15-MHz ultrasound biomicroscopy (RION Inc., Kokubunji, Tokyo) examinations were performed on all eyes in the outpatient clinic. Color fundus photographs were taken with RetCam (Massie Research Laboratories Inc., Dublin, CA). Fluorescein angiography was performed under general anesthesia using the fluorescein angiography unit of the RetCam just before the sample collection.

The stage of the ROP was classified according to international classification,[15] and the vascular activity was classified as active if the eye had 1) plus disease, 2) new vessels growing into the vitreous at the ridge of a tractional RD area, or 3) combined effusive and tractional RD.[14]

Sample Collection and Measurement of Vascular Endothelial Growth Factor

Aqueous humor was collected under general anesthesia with a 27-gauge needle just before the surgery or intravitreal injection of bevacizumab. The amount of undiluted aqueous humor collected ranged from 0.02 mL to 0.1 mL. The samples were not analyzed at the time of collection, but were stored in a deep freezer at −80°C until use. The concentration of VEGF was measured by enzyme-linked immunosorbent assay using a commercially available kit (Quantikine: R&D Systems Inc., Minneapolis, MN), which measures both human $VEGF_{121}$ and $VEGF_{165}$. There

Table 1. Patient Characteristics and the Concentration of VEGF in Aqueous Humor

Patient No.	Gestational Age (Weeks)	Postmenstrual Age (Weeks)	Age (Months)	VEGF Before or Without Bevacizumab (pg/mL)	VEGF After Bevacizumab (pg/mL)
Control					
1			2	156	
2			2	ND	
3			5	ND	
4			7	158	
Stage 4 ROP					
1	22	39		564	
2	26	37		944	
3R	27	37		1,750	
3L	27	37		1,890	
4*	24	64		184	
5	25	41†			60 (4 days‡)
6	22	35, 36†		395	ND (4 days‡)
Stage 5 ROP					
7	28	40, 41†		1,990	230 (7 days‡)
8L	23	36, 43†		5,050	290 (48 days‡)
8R*	23	45		370	

*Inactive.
†Postmenstrual age when aqueous humor was collected after bevacizumab injection.
‡Days after bevacizumab injection.
ND, not detectable.

were three samples in which the VEGF was not detectable. However, as the amount of the samples collected from each eye was different and less than 0.2 mL, the minimum amount necessary for the test, all of the samples had to be diluted with Calibrator Diluent RD6U before use. The sample from Control 2 was diluted 10×, Control 3 was diluted 4×, and ROP 6 after bevacizumab was diluted 5× before the measurement. Thus, the concentration of VEGF in these eyes, in which VEGF was not detectable, might have been higher than 31 pg/mL, the minimum detectable limit of this kit.

Results

The concentration of VEGF in the aqueous humor of 1 of the eyes with congenital cataract was 158 pg/mL, and it was less than the detection level in the other 2 eyes. The concentration in an eye with a persistent pupillary membrane was 156 pg/mL.

The concentration of VEGF in 10 eyes with ROP ranged from 184 to 5,050 pg/mL, which is approximately 1.2× to 32× higher than that in the control eyes (Figure 1). Aqueous humor was collected from seven eyes at Stage 4 and three eyes at Stage 5. One eye at Stage 4 and one at Stage 5 were vascularly inactive. The mean concentration of VEGF in the vascularly active ROP was 1,109 pg/mL in the 5 Stage 4 eyes (395, 564, 944, 1,750, and 1,890 pg/mL in the Stage 4 eyes), and 3,520 pg/mL in the 2 Stage 5 eyes (1,990 and 5,050 pg/mL). In the vascularly inactive eyes, the VEGF level was 184 pg/mL in the 1 Stage 4 eye and 370 pg/mL in 1 Stage 5 eye. Thus, the concentration of VEGF in the vascularly active eyes tended to be higher than in inactive eyes, although statistical analysis could not be performed due to the small number of eyes (Figure 1).

Bevacizumab was injected into six active ROP eyes, four at Stage 4 and two at Stage 5, and aqueous humor was collected from two Stage 4 and two Stage 5 eyes 4 to 48 days after the injection just before vitrectomy. In the Stage 4 eyes, the concentration of

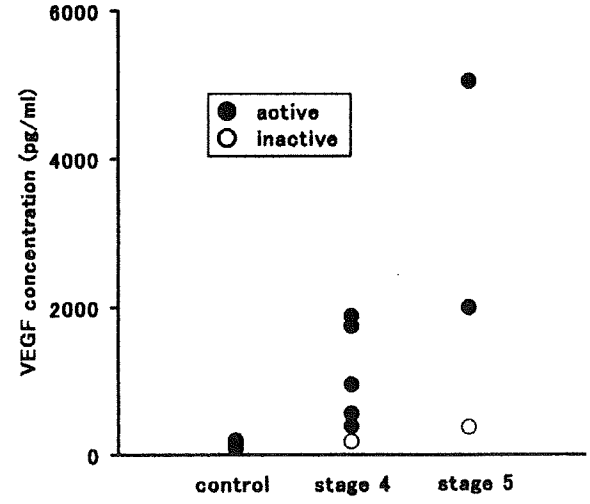

Fig. 1. Concentration of vascular endothelial growth factor (VEGF) in the aqueous humor without or before bevacizumab injection in Stages 4 and 5 ROP and control eyes are shown.

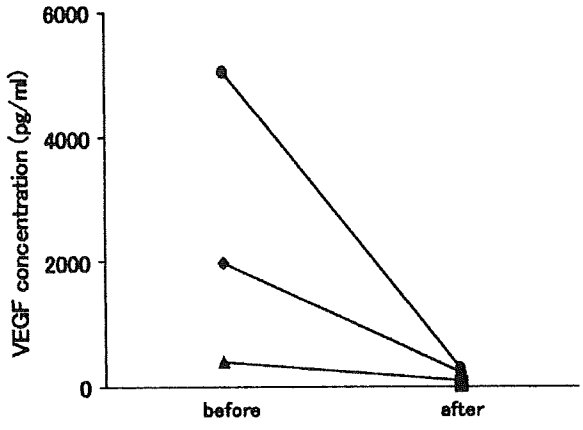

Fig. 2. Vascular endothelial growth factor (VEGF) in the aqueous humor before and/or after bevacizumab injection. The concentration of VEGF in four ROP eyes that had a bevacizumab injection is shown. The concentration before (right) and after (left) injection was measured in three eyes, and after injection in one eye.

unbound VEGF was not detected in 1 eye, and was 60 pg/mL in the other eye 4 days after the injection. In 1 stage 5 eye, the concentration decreased to 230 pg/mL, 7 days after the injection. For 1 Stage 5 eye, vitrectomy was postponed because the patient developed chronic lung disease, and vitrectomy could be safely performed 48 days after the bevacizumab injection. The concentration of VEGF at that time was 290 pg/mL (Figure 2). Fourteen days later, vitrectomy was also performed on the fellow eye without bevacizumab injection, and the concentration of VEGF was 370 pg/mL. The concentration of the VEGF after bevacizumab injection was significantly lower than that of active ROP eyes (145 versus 1,460; $P = 0.04$ with Mann–Whitney U test. The level of VEGF in nondetectable samples was set to 31 pg/mL for statistical analysis). The concentration of VEGF after bevacizumab injection was not measured in two eyes, because the retina was reattached by scleral buckling that was performed together with the injection of bevacizumab, and vitrectomy was not necessary.

Fluorescein angiography was performed before and after the intravitreal injection of bevacizumab in two eyes. In these eyes, there was a considerable decrease of fluorescein leakage from the new vessels after the injection of bevacizumab (Figure 3A and B).

All of the Stage 4 eyes injected with bevacizumab were Stage 4B, and the retina of the two eyes was reattached with one or two vitrectomies without silicon oil tamponade (Figure 3C–F), and two eyes with single encircling surgery (Figure 3G and H). One Stage 5 eye underwent vitrectomy 48 days after the injection, and the retina was reattached under silicon oil (Figure 3I and J). However, one Stage 5 eye with multiple retinal breaks required three surgeries for the retina to be reattached under silicon oil. The silicon oil removal is still being considered for these two eyes.

No ocular complications, such as endophthalmitis, new retinal breaks, or any obvious systemic side effects that were related to bevacizumab were observed.

Comments

The concentration of VEGF in the aqueous humor of eyes at advanced stages of ROP was very high and was higher than that of eyes of adults with PDR (1,460 versus 524; $P = 0.01$ with Mann–Whitney U test) and eyes of infants <1 year without retinal disorders (1,460 versus 94; $P = 0.01$ with Mann–Whitney U test). In these statistical analyses, samples with nondetectable levels of VEGF were set to 31 pg/mL.

Because the concentration of VEGF in the aqueous humor was correlated with the grade of diabetic retinopathy,[16] it would be interesting to know whether there was also a correlation between the VEGF concentration and stage of ROP. Our results showed that the mean VEGF concentration in the Stage 5 eyes was 3× higher than that in the Stage 4 eyes, and one eye at Stage 5 had a level of 5,050 pg/mL. Only three eyes at Stage 4 had <1,000 pg/mL of VEGF. However, Lashkari et al[13] reported that the concentration of VEGF in the subretinal fluid in Stage 4 eyes did not differ significantly from that of Stage 5 ROP eyes. This difference from our results was probably because of the difference in the site where the sample was collected, viz, the aqueous humor or the subretinal fluid. Another reason that might account for this difference might be whether the vessels were active or inactive. Lashkari et al did not report the vascular status of their eye, and it may have been at the vascularly inactive ROP stage. Sonmez et al[14] classified Stage 4 ROP into vascularly active or vascularly inactive state, and reported that the level of VEGF was higher in the active group than in the inactive group as we have found. However, the number of eyes tested in our study was limited, and statistical analysis was not performed. Thus, we cannot make a conclusion on this question.

The intravitreal injection of bevacizumab decreased the concentration of VEGF in the aqueous humor of Stage 4 and Stage 5 ROP eyes markedly, and the concentration decreased to 60, 230, and 290 pg/mL and the level was not detectable in one eye (direct statistical comparison, before and after injection, was not performed because of the small number of the eyes), which is comparable with that of the control eyes of infants. However, it was still higher than that in eyes with PDR after bevacizumab injections reported previously.[10] The concentration in all of these

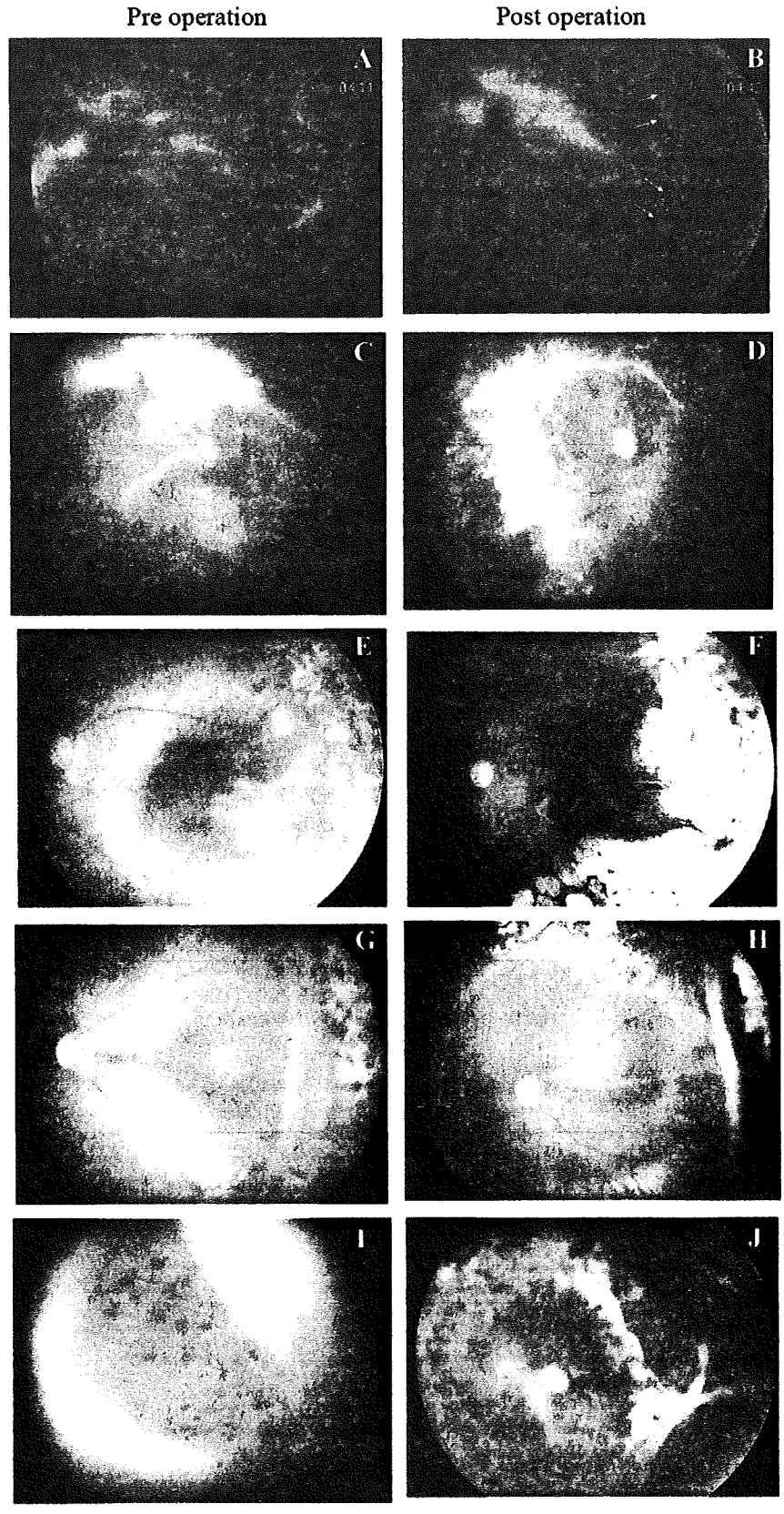

Fig. 3. Clinical outcome of the eyes treated with bevacizumab. (**A–D**) Patient 5 (Stage 4, Table 1). Retina was totally detached except the peripheral retina (**A** and **C**) and bevacizumab was injected as a preoperative adjunctive therapy at postmenstrual age of 40 weeks. Four days after injection, decrease of fluorescence leakage (arrow) was observed (**B**) and vitrectomy with lensectomy was performed. One month later, second membrane removal operation was performed, and retina was totally reattached (**D**). The visual acuity of this eye is LS (+) 1 year after the second surgery may be due to the good vision of the fellow eye, and the vision training is performed. (**E** and **F**) Patient 6 (Stage 4, Table 1). Because of the strong proliferation of active new vessels, bevacizumab was injected as preoperative adjunctive therapy at the postmenstrual age of 35 week (**E**). Four days after injection, vitrectomy with lensectomy was performed, and the retina was totally reattached. Four months after operation, macular is formed (**F**) and vision tracking is obtained. (**G** and **H**) Patient 2 (Stage 4, Table 1). Encircling surgery was performed at postmenstrual age of 35 weeks, but as the vascular activity was high and the retinal detachment remained (**G**), vitrectomy was planned. However, after the bevacizumab injection at 14 days after the encircling procedure, the progression stopped and the retina was reattached. Six months after the injection, the macular configuration was present (**H**) and visual acuity of 0.75 cycles/degree (Teller Acuity Cards) was obtained. (**I** and **J**): Patient 8L (Stage 5, Table 1). At postmenstrual age of 36 weeks, the retina was totally detached to closed funnel shape with multiple retinal breaks (**I**). Bevacizumab was injected, but vitrectomy was postponed because of the chronic lung disease. Vitrectomy with lensectomy was performed 48 days after the bevacizumab injection at the postmenstrual age of 43 weeks, and silicon oil was injected because of the retinal break. One year after the operation, the retina is reattached (**J**), and silicone oil removal is considered.

eyes was below the detection level of 31 pg/mL (no statistical analysis was performed). This difference might be because the VEGF concentration before the injection was much higher in the eyes with ROP, or the amount of bevacizumab injected in PDR eyes was greater. However, because the assays were run by different methods, at different institutes, and at different times, it might not be proper to compare these results. Although there was detectable VEGF remaining in some eyes, it was decided not to increase the amount of bevacizumab for these infants because we did observe a decrease of fluorescein leakage after the injection and less bleeding during vitrectomy with this dosage, and because of the possible systemic side effects. It also is possible that the residual level of VEGF might have prevented the topical side effects, e.g., obstruction of the development of normal vessels and neural retina, as the level is similar to that of control eyes, although the distribution of VEGF might be different from normal.

One Stage 5 eye became vascularly inactive and its VEGF level was 370 pg/mL, 62 days after the bevacizumab was injected into the fellow eye. However, it is not clear whether this was due to circulating bevacizumab or just a natural course of ROP. Because there was no ROP eye in which samples were collected twice in 4 or 7 days without bevacizumab as control, there is a possibility that decrease in ocular VEGF in other bevacizumab injected eyes can be the natural course of this disease. However, as a rapid inactivation of ROP was observed in these eyes and bevacizumab is shown to decrease VEGF in other diseases such as PDR,[10] this rapid decrease of VEGF is likely to be the effect of this drug.

From August 2004 to November 2006, vitrectomy was performed for Stage 4B (3 eyes) and Stage 5 (17 eyes) eyes without bevacizumab injection at our hospital. The average postmenstrual age of these infants was 49.7 weeks (38–67 weeks). Without bevacizumab, vitrectomy was performed 2.1 ± 0.9 times/eye (1–5 times), and the rate of reattachment was 55%. However, vitrectomy could be performed on the eyes treated with bevacizumab without severe bleeding during membrane removal at postmenstrual age of 40.3 weeks (36–43 weeks) which is earlier than that without bevacizumab, without severe bleeding during membrane removal. In two Stage 4B eyes, reattachment of the retina was obtained without silicon oil tamponade with one or two surgeries, and one Stage 5 eye, reattachment of the retina under silicon oil was obtained with one surgery. The removal of the silicon oil is being considered. For one Stage 5 eye with multiple retinal breaks, reattachment of the retina under silicon oil was obtained with three surgeries, and removal of the silicon oil is still being considered. Moreover, two Stage 4B eyes, which received an injection of bevacizumab just before or 2 weeks after encircling surgery, had a reattachment of the retina without additional operations. From August 2004 to November 2006, encircling surgery was performed without bevacizumab at our hospital for two Stage 4B eyes, but both eyes progressed to Stage 5, and vitrectomy was required for reattachment. These results suggest that bevacizumab injection might be useful adjunctive therapy for both vitrectomy and encircling surgery for severe ROP, although the number of the eyes studied was very limited.

In conclusion, an intravitreal injection of bevacizumab decreased the VEGF level markedly in the aqueous humor of ROP eyes although a direct comparison, before and after injection, was not performed statistically. However, the concentration of VEGF was not below the detection level in most of the eyes after injection. Our findings indicate that bevacizumab might be useful for preoperative adjunctive therapy for ROP, however the number of eyes studied was very limited and further studies are needed.

Key words: retinopathy of prematurity, vascular endothelial growth factor, bevacizumab, intravitreal injection, aqueous humor.

Acknowledgment

The authors thank Dr. Duco Hamasaki for critical reading of the manuscript.

References

1. Ferrara N, Davis-Smyth T. The biology of vascular endothelial growth factor. Endocr Rev 1997;18:4–25.
2. Aiello LP, Avery RL, Arrigg PG, et al. Vascular endothelial growth factor in ocular fluid of patients with diabetic retinopathy and other retinal disorders. N Engl J Med 1994;331:1480–1487.
3. Adamis AP, Miller JW, Bernal MT, et al. Increased vascular endothelial growth factor levels in the vitreous of eyes with proliferative diabetic retinopathy. Am J Ophthalmol 1994;118:445–450.
4. Stone J, Itin A, Alon T, et al. Development of retinal vasculature is mediated by hypoxia-induced vascular endothelial growth factor (VEGF) expression by neuroglia. J Neurosci 1995;15(7 Pt 1):4738–4747.
5. Ferrara N. Vascular endothelial growth factor as a target for anticancer therapy. Oncologist 2004;9(Suppl 1):2–10. Review.
6. Rosenfeld PJ, Schwartz SD, Blumenkranz MS, et al. Maximum tolerated dose of a humanized anti-vascular endothelial growth factor antibody fragment for treating neovascular age-related macular degeneration. Ophthalmology 2005;112:1048–1053.
7. Rosenfeld PJ, Moshfeghi AA, Puliafito CA. Optical coherence tomography findings after an intravitreal injection of bevacizumab (avastin) for macular edema from central retinal vein occlusion. Ophthalmic Surg Lasers Imaging 2005;36:331–335.
8. Avery RL, Pearlman J, Pieramici DJ, et al. Intravitreal bevacizumab (Avastin) in the treatment of proliferative diabetic retinopathy. Ophthalmology 2006;113:1695.e1–e15.

9. Chen E, Park CH. Use of intravitreal bevacizumab as a preoperative adjunct for tractional retinal detachment repair in severe proliferative diabetic retinopathy. Retina 2006;26:699–700.
10. Sawada O, Kawamura H, Kakinoki M. Vascular endothelial growth factor in aqueous humor before and after intravitreal injection of bevacizumab in eyes with diabetic retinopathy. Arch Ophthalmol 2007;125:1363–1366.
11. Hiraoka M, Watanabe T, Kawakami T, et al. Retinopathy of prematurity in extremely low birth weight infants: a Tokyo multicenter study. Nippon Ganka Gakkai Zasshi 2004;108: 600–605.
12. Chung EJ, Kim JH, Ahn HS, et al. Combination of laser photocoagulation and intravitreal bevacizumab (Avastin) for aggressive zone I retinopathy of prematurity. Graefes Arch Clin Exp Ophthalmol 2007;245:1727–1730.
13. Lashkari K, Hirose T, Yazdany J, et al. Vascular endothelial growth factor and hepatocyte growth factor levels are differentially elevated in patients with advanced retinopathy of prematurity. Am J Pathol 2000;156:1337–1344.
14. Sonmez K, Drenser KA, Caoine A Jr. et al. Vitreous levels of stromal cell-derived factor 1 and vascular endothelial growth factor in patients with retinopathy of prematurity. Ophthalmology 2008;115:1065–1070.e1.
15. ICROP Committee for Classification of Late stages ROP. An international classification of retinopathy of prematurity, II: the classification of retinal detachment. Arch Ophthalmol 1987;105:906–912.
16. Funatsu H, Yamashita H, Noma H, et al. Risk evaluation of outcome of vitreous surgery based on vitreous levels of cytokines. Eye 2007;21:377–382.

Neuroscience Letters 462 (2009) 267–271

Contents lists available at ScienceDirect

Neuroscience Letters

journal homepage: www.elsevier.com/locate/neulet

A novel missense mutation (Leu46Val) of *PAX6* found in an autistic patient

Motoko Maekawa[a,*], Yoshimi Iwayama[a], Kazuhiko Nakamura[b], Miho Sato[c], Tomoko Toyota[a], Tetsuo Ohnishi[a], Kazuo Yamada[a], Taishi Miyachi[d], Masatsugu Tsujii[d,e], Eiji Hattori[a], Nobuo Maekawa[f], Noriko Osumi[g,h], Norio Mori[b], Takeo Yoshikawa[a,h]

[a] *Laboratory for Molecular Psychiatry, RIKEN Brain Science Institute, 2-1 Hirosawa, Wako, Saitama 351-0198, Japan*
[b] *Department of Psychiatry and Neurology, Hamamatsu University School of Medicine, Shizuoka, Japan*
[c] *Department of Ophthalmology, Hamamatsu University School of Medicine, Shizuoka, Japan*
[d] *The Osaka-Hamamatsu Joint Research Center for Child Mental Development, Hamamatsu University School of Medicine, Shizuoka, Japan*
[e] *Faculty of Sociology, Chukyo University, Toyota, Japan*
[f] *Maekawa Eye Clinic, Miyagi, Japan*
[g] *Department of Developmental Neurobiology, Tohoku University Graduate School of Medicine, Miyagi, Japan*
[h] *CREST, Japanese Science and Technology Agency, Tokyo, Japan*

ARTICLE INFO

Article history:
Received 28 May 2009
Received in revised form 3 July 2009
Accepted 6 July 2009

Keywords:
PAX6
Missense mutation
Autism
Aniridia

ABSTRACT

The paired box 6 (PAX6) is a transcription factor expressed early in development, predominantly in the eye, brain and pancreas. Mutations in *PAX6* are responsible for eye abnormalities including aniridia, and it is also known that some *PAX6* mutations result in autism with incomplete penetrance. We resequenced all the exons and flanking introns of *PAX6* in 285 autistic patients in the Japanese, with the possibility that novel mutations may underlie autism. Fifteen different polymorphisms were identified: 13 are novel, and 2 were previously reported (rs667773 and rs3026393). Among the novel ones, there is one missense mutation that was found in a patient: 136C > G (Leu46Val) (single nucleotide polymorphism ID "ss130452457" is temporarily assigned). Leu46 is extremely conserved from fly to human, and we did not detect Val46 in 2120 nonautistic subjects. The autistic patient carrying this heterozygous mutation showed reduced vision, photophobia and eyelid ptosis, but no other ocular abnormality such as aniridia. Our findings suggest the necessity of further studies on the causal relationship between *PAX6* and autism.

The human paired box 6 (*PAX6*) gene is located on chromosome 11p13, and its orthologues have been found in diverse species. This gene encodes a transcription factor that is involved in multiple developmental pathways and is expressed early in the development of the eye, numerous regions of the brain, and the pancreas [25]. The *PAX6* gene of 22 kb size contains 14 exons, including an alternatively spliced exon 5a that encodes 14 amino acids, and encodes a protein of 422 amino acid (Fig. 1). The PAX6 protein contains two DNA-binding domains (one paired domain and one homeodomain), and one proline/serine/threonine-rich (PST) transactivation domain. PAX6 affects the development of the nervous system and brain by regulating proneural genes such as neurogenin 2 (*Ngn2*) and achaete–scute complex homolog-like 1 (*Mash-1*) [28,36]. The *Pax6* heterozygous mutant mice and rats, i.e., "*small eye*", show both ocular and neuronal phenotypes including an absent olfactory bulb, a decrease in the number of cortical neurons and cortical plate thickness, as well as altered dorsoventral patterning of the forebrain, and a decrease in hippocampal neurogenesis at the postnatal stage [18].

In human, in addition to the reports of associations of various *PAX6* mutations with eye abnormalities including syndromic ones like Peters anomaly [8,26], there is emerging evidence of the roles of *PAX6* mutations in behavioral and neurodevelopmental disease phenotypes such as autism and mental retardation. For instance, recent studies have identified individuals with *PAX6* mutations who manifest mental retardation and aniridia [12,20,32]. In addition, magnetic resonance imaging (MRI) studies of patients with aniridia have shown subtle brain abnormalities including a lack of the anterior commisure and pineal gland [23]. These accumulating lines of evidence suggest that concomitant phenotypes are determined by the nature of *PAX6* mutations. In this study, we carried out resequencing analysis of the gene in autistic patients with, with the aim of searching for additional mutations of *PAX6*, which might be associated with the disease.

Two hundred and eighty-five autistic patients of Japanese descent (236 men, 49 women; age, from 3 to 32 years old) were analyzed. The diagnosis of autism was made on the basis of the Autism Diagnostic Interview-Revised (ADI-R) criteria [17] with consensus from at least two experienced psychiatrists. All available medical

* Corresponding author. Tel.: +81 48 467 5968; fax: +81 48 467 7462.
E-mail address: mmaekawa@brain.riken.jp (M. Maekawa).

0304-3940/$ – see front matter © 2009 Elsevier Ireland Ltd. All rights reserved.
doi:10.1016/j.neulet.2009.07.021

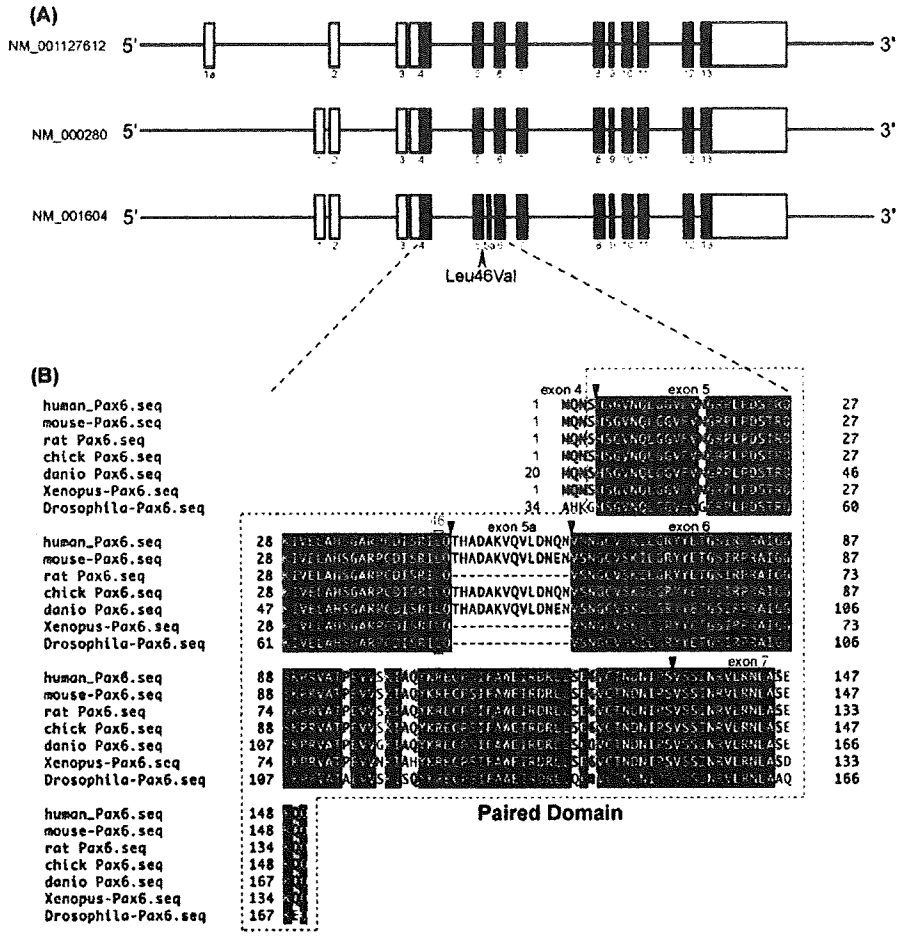

Fig. 1. Genomic structure of human *PAX6* and amino acid sequences of PAX6/Pax6. (A) Genomic structure and location of 136G (Val46) missense mutation for human *PAX6*. Exons are denoted by boxes, with untranslated regions in white and translated regions in black. A black arrowhead indicates the location of the missense mutation. Note that the three isoforms are shown (http://genome.ucsc.edu/cgi-bin/hgGateway?org=human). (B) Amino acid sequence alignments of PAX6/Pax6 among species. The black boxes indicate the conserved amino acids from Drosophila to human. The grey boxes show the partially conserved ones. The conserved 46Leu is indicated by a red square. The red-broken-line box shows the paired domain that contains the conventional 128 residues [34] and five subsequent residues (SEKQQ) [38]. (For interpretation of the references to color in this figure caption, the reader is referred to the web version of the article.)

records were also taken into consideration. Regarding a detected missense mutation in patient samples, we analyzed 2120 nonautistic subjects, who are 1060 patients with schizophrenia (503 men, 557 women; mean age 48.0 ± 13.8 years) and 1060 controls who are free of mental disorders (503 men, 557 women; mean age 47.7 ± 13.6 years) [16]. All the subjects were from central Japan. The study was approved by the ethics committees of RIKEN and Hamamatsu University and was conducted in accordance with the Declaration of Helsinki (http://www.wma.net). All the participants provided written informed consent (for patients under 16 years old, we explained the aim of this study to the patients' parents and as long as possible to the patients in easy terms, and obtained written informed consent from at least their parents).

Genomic DNA was isolated from blood samples by standard methods. All the exons and exon/intron boundaries of *PAX6* were screened for polymorphisms by direct sequencing of polymerase chain reaction (PCR) products. The primers used for amplification are listed in Supplementary Table 1. PCR was performed with an initial denaturation at 95 °C for 10 min, followed by 35 cycles at 95 °C for 15 s, 60–63 °C (optimized for each primer pair) for 15 s, 72 °C for 30 s, and a final extension at 72 °C for 10 min, with AmpliTaqGold (Applied Biosystems, Foster City, CA) or it was performed with an initial denaturation at 98 °C for 5 min, followed by 35 cycles at 98 °C for 45 s, 58–61 °C for 30 s, 68 °C for 30 s, and a final extension at 68 °C for 10 min, with Pwo SuperYield DNA Polymerase (Roche, Basel, Switzerland). Direct sequencing of PCR products was performed with the BigDye Terminator v3.1 Cycle Sequencing kit (Applied Biosystems) and the ABI PRISM 3730*xl* Genetic Analyzer (Applied Biosystems). Polymorphisms were detected with the SEQUENCHER program (Gene Codes Corporation, Ann Arbor, MI). The genomic structure of *PAX6* is based on the UCSC March 2006 draft assembly of the human genome database (http://www.genome.ucsc.edu), and the NCBI (http://www.ncbi.nlm.nih.gov/) database was searched for known single nucleotide polymorphisms (SNPs). Custom TaqMan SNP Genotyping assays (Applied Biosystems) were used to score the identified missense SNP by the TaqMan assay method [27], and using ABI PRISM 7900 Sequence Detection System (SDS) and SDS v2.3 software (Applied Biosystems).

Our polymorphism screening detected a total of 15 different variants in the *PAX6*: 13 are novel (−11,521C > T, IVS4-85T > C, IVS4-70~−72Ins/DelTCT, IVS4-42C > T, 117G > A, 136C > G, IVS5-163C > T, 319C > T, IVS6 + 28C > T, IVS8 + 14Ins/DelT, 867T > C, IVS12 + 11G > A and 1194C > T), and 2 were previously reported (rs667773 and rs3026393) (Table 1). With respect to novel variants, the 136C > G was a missense mutation (Leu46Val; ss130452457) located in the paired domain, which was found in one patient as a heterozygote (Table 1 and Fig. 1). We then examined 2120 nonautistic subjects for this missense mutation. However, the mutation was not detected

Table 1
PAX6 polymorphisms detected in 285 autistic patients in the Japanese.

Polymorphism[a]	dbSNP ID	Allele frequency
ATG~−11,521C>T	Novel	1/570
IVS4-85T>C	Novel	1/570
IVS4-70~72Ins/DelTCT	Novel	1/570
IVS4-42C>T	Novel	1/570
117G>A [Pro(CCG)39Pro(CCA)]	Novel	1/570
136C>G [Leu(CTG)46Val(GTG)]	Novel	1/570
IVS5-163C>T	Novel	1/570
319C>T [Leu(CTG)107LeuTTG]	Novel	1/570
IVS6+28C>T	Novel	1/570
IVS8+14Ins/DelT	Novel	1/570
IVS9-12C>T	rs667773	68/570
867T>C [Ser(AGT)289Ser(AGC)]	Novel	4/570
IVS12+11(G>A)	Novel	1/570
IVS12+43T>G	rs3026393	261/570
1194C>T [Ser(TCC)398Ser(TCT)]	Novel	4/570

[a] Major allele > minor allele; intron Nos. are based on the NM_000280 (Fig. 1A).

in these subjects. We also examined 252 Autism Genetic Resource Exchange (AGRE) trios (756 samples; http://www.agre.org), but again did not detect it.

The autistic patient with the *PAX6* missense mutation (Leu46Val) is a daughter of nonconsanguineous parents (Fig. 2), and the mutation was transmitted from her father. However, her father does not have autism, major depression, anxiety and social awkwardness implying a sign of autism upon psychiatric interview, as well as her mother and older brother. The patient's pregnancy and birth history were without any problems. At 1.5 years of age, she was assessed as developing normally except for mild speech delay. During her preschool days, she used to spend many hours playing alone. She attended a normal elementary school and a normal junior high school. However, she attended a high school for handicapped children because of her difficulty in learning at a normal high school. When she was 10 years old, she was diagnosed as having autism by an expert in childhood psychiatry. She had deficits in all three areas of communication, reciprocal social interaction and behavior. Her ADI-R scores were 17 in the social domain (cutoff = 10), 15 in the language (verbal) domain (cutoff = 8), and 6 in the repetitive/restrictive behaviors domain (cutoff = 3). The Wechsler Intelligence Scale was administered with a full-scale WISC-III of 66 (verbal IQ 73, performance IQ 67). She sometimes looked anxious, which manifested intermittently and briefly. Therefore, she was administered psychotropic drugs from 10 years of age. She had no histories of any other neurological illnesses including seizure and head injury. In addition, MRI examination revealed normal morphologies of the corpus callosum, anterior commissure, grey matter in anterior cingulate cortex, medial temporal lobe, olfactory bulb, pineal gland and cerebellum. The blood karyotype analysis result was also normal and "fragile X" was excluded. With respect to ocular phenotypes, the patient displayed reduced vision, photophobia and eyelid ptosis, but no other ocular abnormalities including aniridia. Her father carrying the same mutation did not show abnormal ocular phenotypes except for reduced vision and age-related macular degeneration (Fig. 3). Recently it is also known that PAX6 regulates proinsulin processing and glucose metabolism via modulation of PC1/3 production [37]. Therefore, we also checked blood glucose levels and BMIs (body mass indexes) of the patient and her father (the patient's BMI is 16.8 and her father's BMI is 22.4), and these measures were within normal limits.

Val46 is deemed to elicit functional impairment, because Leu46 is conserved from Drosophila to human (Fig. 1) and Leu46Arg and Leu46Pro mutations are reported to affect ocular phenotypes in previous studies [5,7]. Additionally, this mutation may be important for the following reasons: (1) the Leu46Val mutation is located in the paired domain, (2) structural analysis of this mutation using the Sequence Analysis Software "GENETYX" (GENETYX Co., Tokyo, Japan) suggests that it may disrupt the helix-turn-helix motif, and as a consequence the DNA-binding properties of the resulting mutated protein may vary, (3) this variant is predicted to be possibly damaging using a tool-website "PolyPhen" that can estimate the possible impact of an amino acid substitution on the structure and function of a protein (http://coot.embl.de/PolyPhen/), and (4) it is also possible that this mutation may exert its effect by disrupting the activity of an exonic splicing enhancer (ESE), because the SC35 score matrix of this mutation (3.17473) is lower than that of the wild type (4.09004), which is calculated using a tool-website "ESE finder" (an online resource to identify ESEs in query sequences) (http://rulai.cshl.edu/cgi-bin/tools/ESE3/esefinder.cgi?process=home). Therefore, these predicted functional consequences may be relevant to the autism phenotype, although the cosegregation was not observed in the present nuclear family.

A network of protein–protein interactions underlies complex biological processes. We addressed this issue using the Genome Network Platform (http://genomenetwork.nig.ac.jp/). There are 36 proteins that can interact with Pax6 and it is reported that 5 proteins out of the 36 proteins correlate with autism, which include HoxB1 [15,22], Tbp [6,31], Diaph1 [24,33], Ifi16 [1,11] and Ep300 [14,29] (Supplementary Fig. 1). For example, Hoxb1 that plays an important role in morphogenesis in all multicellular organisms can interact with both the paired domain and homeodomain of Pax6

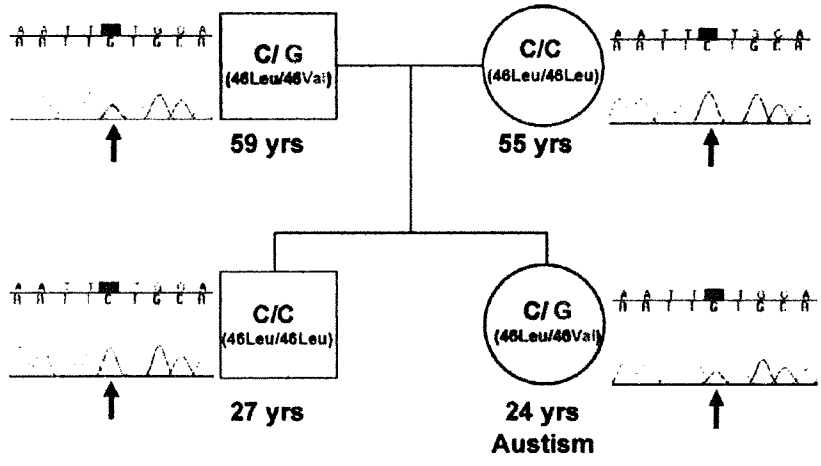

Fig. 2. Family structure of a patient with the *PAX6* missense mutation. Grey symbols indicate individuals carrying heterozygous *PAX6* Val46 allele. White symbols show the subjects with homozygous Leu46 alleles. Squares represent men and circles represent women. Genotype and sequence electrophelogram of each subject are also shown.

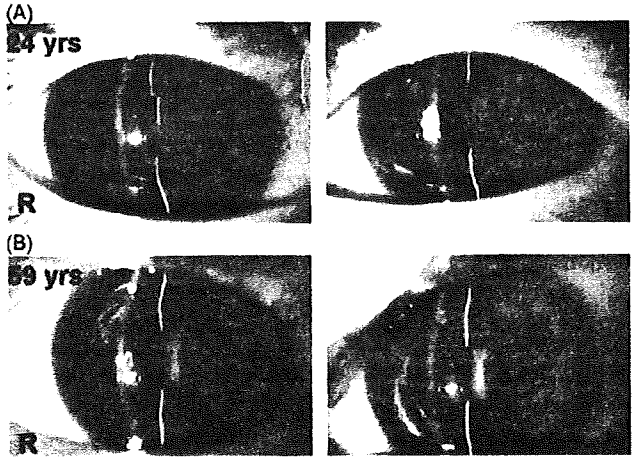

Fig. 3. Biomicroscopic observations of autistic patient (A) and her father (B) both of whom carry the mutant allele. (A) and (B) show the slit lamp aspects of ocular anterior segments as well as the lens of the subjects. Ages are also shown. R, right eye; L, left eye.

and can enhance Pax6-mediated transactivation of a minimal promoter that contains consensus Pax6 paired domain binding sites in *in vitro* experiments [22]. The Leu46Val missense mutation was located in the paired domain of PAX6. Therefore, the mutated PAX6 may affect the autism phenotype, owing to the attenuated interaction with HOXB1.

Concerning the penetrance of *PAX6* mutations in aniridia, it is known that *PAX6* missense mutations are a less frequent cause than expected [35], and they are not fully penetrant for other ocular anomalies [8]. Our current results that the Val46 allele did not cosegregate with autism or ocular phenotype in the family suggest that the Val46 of PAX6 may have only a modest effect, if any, on the development of autism and ocular abnormalities. It is also of note that in general autism is a multi-factorial disease caused by multiple susceptibility genes of small effect sizes, environmental factors and their interactions like other psychiatric illnesses [4].

MRI and functional MRI (fMRI) show that individuals with *PAX6* heterozygous mutations (haploinsufficiency) have structural abnormalities of grey matter in the anterior cingulated cortex, cerebellum and medial temporal lobe, as well as white matter deficits in the corpus callosum [9,10,13,23,30]. Additionally, patients of high-functioning autism with *PAX6* mutations (not haploinsufficiency) also have significant structural abnormalities [2,3,7]. In this study, we did not detect any abnormal brain structures in the patient. However, we previously reported that hippocampal neurogenesis is reduced in the *Pax6* heterozygous mutant rats that present behavioral abnormalities including decreased prepulse inhibition [18,19]. Therefore, we suspect that the autistic patient with the *PAX6* missense mutation may also have suffered from dampened hippocampal neurogenesis, potentially contributing to autism as one of the risk-conferring events [21].

In summary, we identified in this study a novel missense mutation of *PAX6* in one autistic patient with mild ocular abnormalities, and the mutation was not detected in 2120 nonautistic subjects. Further studies using larger samples and on the biological importance of this missense mutation are required.

Acknowledgements

We thank Dr. Yujiro Yoshihara for MRI inspection. We acknowledge the support of the Autism Genetics Resource Exchange (AGRE, http://www.agre.org) for the samples and thank the members of the Research Resource Center of the RIKEN Brain Science Institute for the sequencing and GeneScan genotyping services. This work was supported by RIKEN BSI Funds, grants from the Ministry of Education Culture, Sports, Science and Technology, the pharmacopsychiatry research grant from the Mitsubishi Pharma Research Foundation, a donation from the Maekawa Incorporated Medical Institution and CREST funds from the Japan Science and Technology Agency.

Appendix A. Supplementary data

Supplementary data associated with this article can be found, in the online version, at doi:10.1016/j.neulet.2009.07.021.

References

[1] B. Asefa, J.M. Dermott, P. Kaldis, K. Stefanisko, D.J. Garfinkel, J.R. Keller, p205, a potential tumor suppressor, inhibits cell proliferation via multiple pathways of cell cycle regulation, FEBS Lett. 580 (2006) 1205–1214.
[2] D.E. Bamiou, N.G. Campbell, F.E. Musiek, R. Taylor, W.K. Chong, A. Moore, V. van Heyningen, S. Free, S. Sisodiya, L.M. Luxon, Auditory and verbal working memory deficits in a child with congenital aniridia due to a PAX6 mutation, Int. J. Audiol. 46 (2007) 196–202.
[3] D.E. Bamiou, S.L. Free, S.M. Sisodiya, W.K. Chong, F. Musiek, K.A. Williamson, V. van Heyningen, A.T. Moore, D. Gadian, L.M. Luxon, Auditory interhemispheric transfer deficits, hearing difficulties, and brain magnetic resonance imaging abnormalities in children with congenital aniridia due to PAX6 mutations, Arch. Pediatr. Adolesc. Med. 161 (2007) 463–469.
[4] D.V. Bishop, Genes, cognition, and communication: insights from neurodevelopmental disorders, Ann. N. Y. Acad. Sci. 1156 (2009) 1–18.
[5] L.Y. Chao, R. Mishra, L.C. Strong, G.F. Saunders, Missense mutations in the DNA-binding region and termination codon in PAX6, Hum. Mutat. 21 (2003) 138–145.
[6] A. Cvekl, F. Kashanchi, J.N. Brady, J. Piatigorsky, Pax-6 interactions with TATA-box-binding protein and retinoblastoma protein, Invest. Ophthalmol. Vis. Sci. 40 (1999) 1343–1350.
[7] A. Dansault, G. David, C. Schwartz, C. Jaliffa, V. Vieira, G. de la Houssaye, K. Bigot, F. Catin, L. Tattu, C. Chopin, P. Halimi, O. Roche, N. Van Regemorter, F. Munier, D. Schorderet, J.L. Dufier, C. Marsac, D. Ricquier, M. Menasche, A. Penfornis, M. Abitbol, Three new PAX6 mutations including one causing an unusual ophthalmic phenotype associated with neurodevelopmental abnormalities, Mol. Vis. 13 (2007) 511–523.
[8] L.K. Davis, K.J. Meyer, D.S. Rudd, A.L. Librant, E.A. Epping, V.C. Sheffield, T.H. Wassink, Pax6 3′ deletion results in aniridia, autism and mental retardation, Hum. Genet. 123 (2008) 371–378.
[9] Z. Ellison-Wright, I. Heyman, I. Frampton, K. Rubia, X. Chitnis, I. Ellison-Wright, S.C. Williams, J. Suckling, A. Simmons, E. Bullmore, Heterozygous PAX6 mutation, adult brain structure and fronto-striato-thalamic function in a human family, Eur. J. Neurosci. 19 (2004) 1505–1512.
[10] G. Estivill-Torrus, T. Vitalis, P. Fernandez-Llebrez, D.J. Price, The transcription factor Pax6 is required for development of the diencephalic dorsal midline secretory radial glia that form the subcommissural organ, Mech. Dev. 109 (2001) 215–224.
[11] K. Garbett, P.J. Ebert, A. Mitchell, C. Lintas, B. Manzi, K. Mirnics, A.M. Persico, Immune transcriptome alterations in the temporal cortex of subjects with autism, Neurobiol. Dis. 30 (2008) 303–311.
[12] C. Graziano, A.V. D'Elia, L. Mazzanti, F. Moscano, S. Guidelli Guidi, E. Scarano, D. Turchetti, E. Franzoni, G. Romeo, G. Damante, M. Seri, A de novo nonsense mutation of PAX6 gene in a patient with aniridia, ataxia, and mental retardation, Am. J. Med. Genet. A 143A (2007) 1802–1805.
[13] I. Heyman, I. Frampton, V. van Heyningen, I. Hanson, P. Teague, A. Taylor, E. Simonoff, Psychiatric disorder and cognitive function in a family with an inherited novel mutation of the developmental control gene PAX6, Psychiatr. Genet. 9 (1999) 85–90.
[14] M.A. Hussain, J.F. Habener, Glucagon gene transcription activation mediated by synergistic interactions of pax-6 and cdx-2 with the p300 co-activator, J. Biol. Chem. 274 (1999) 28950–28957.
[15] J.L. Ingram, C.J. Stodgell, S.L. Hyman, D.A. Figlewicz, L.R. Weitkamp, P.M. Rodier, Discovery of allelic variants of HOXA1 and HOXB1: genetic susceptibility to autism spectrum disorders, Teratology 62 (2000) 393–405.
[16] Y. Iwayama, M. Maekawa, K. Yamada, T. Toyota, T. Ohnishi, Y. Iwata, K.J. Tsuchiya, G. Sugihara, M. Kikuchi, K. Hashimoto, M. Iyo, T. Inada, H. Kunugi, N. Ozaki, N. Iwata, S. Nanko, K. Iwamoto, Y. Okazaki, T. Kato, T. Yoshikawa, Association analyses between brain-expressed FABP (fatty-acid binding protein) genes and schizophrenia and bipolar disorder, Neuropsychiatr. Genet. (2009) Jun 24. [Epub].
[17] C. Lord, M. Rutter, A. Le Couteur, Autism diagnostic interview-revised: a revised version of a diagnostic interview for caregivers of individuals with possible pervasive developmental disorders, J. Autism Dev. Disord. 24 (1994) 659–685.
[18] M. Maekawa, N. Takashima, Y. Arai, T. Nomura, K. Inokuchi, S. Yuasa, N. Osumi, Pax6 is required for production and maintenance of progenitor cells in postnatal hippocampal neurogenesis, Genes Cells 10 (2005) 1001–1014.
[19] M. Maekawa, N. Takashima, M. Matsumata, S. Ikegami, M. Kontani, Y. Hara, H. Kawashima, Y. Owada, Y. Kiso, T. Yoshikawa, K. Inokuchi, N. Osumi, Arachi-

donic acid drives postnatal neurogenesis and elicits a beneficial effect on prepulse inhibition, a biological trait of psychiatric illnesses, PLoS One 4 (2009) e5085.
[20] A. Malandrini, F. Mari, S. Palmeri, S. Gambelli, G. Berti, M. Bruttini, A.M. Bardelli, K. Williamson, V. van Heyningen, A. Renieri, PAX6 mutation in a family with aniridia, congenital ptosis, and mental retardation, Clin. Genet. 60 (2001) 151–154.
[21] M.T. Mercadante, R.M. Cysneiros, J.S. Schwartzman, R.M. Arida, E.A. Cavalheiro, F.A. Scorza, Neurogenesis in the amygdala: a new etiologic hypothesis of autism? Med. Hypotheses 70 (2008) 352–357.
[22] I. Mikkola, J.A. Bruun, T. Holm, T. Johansen, Superactivation of Pax6-mediated transactivation from paired domain-binding sites by dna-independent recruitment of different homeodomain proteins, J. Biol. Chem. 276 (2001) 4109–4118.
[23] T.N. Mitchell, S.L. Free, K.A. Williamson, J.M. Stevens, A.J. Churchill, I.M. Hanson, S.D. Shorvon, A.T. Moore, V. van Heyningen, S.M. Sisodiya, Polymicrogyria and absence of pineal gland due to PAX6 mutation, Ann. Neurol. 53 (2003) 658–663.
[24] E.M. Morrow, S.Y. Yoo, S.W. Flavell, T.K. Kim, Y. Lin, R.S. Hill, N.M. Mukaddes, S. Balkhy, G. Gascon, A. Hashmi, S. Al-Saad, J. Ware, R.M. Joseph, R. Greenblatt, D. Gleason, J.A. Ertelt, K.A. Apse, A. Bodell, J.N. Partlow, B. Barry, H. Yao, K. Markianos, R.J. Ferland, M.E. Greenberg, C.A. Walsh, Identifying autism loci and genes by tracing recent shared ancestry, Science 321 (2008) 218–223.
[25] N. Osumi, The role of Pax6 in brain patterning, Tohoku J. Exp. Med. 193 (2001) 163–174.
[26] J. Prosser, V. van Heyningen, PAX6 mutations reviewed, Hum. Mutat. 11 (1998) 93–108.
[27] K. Ranade, M.S. Chang, C.T. Ting, D. Pei, C.F. Hsiao, M. Olivier, R. Pesich, J. Hebert, Y.D. Chen, V.J. Dzau, D. Curb, R. Olshen, N. Risch, D.R. Cox, D. Botstein, High-throughput genotyping with single nucleotide polymorphisms, Genome Res. 11 (2001) 1262–1268.
[28] R. Scardigli, N. Baumer, P. Gruss, F. Guillemot, I. Le Roux, Direct and concentration-dependent regulation of the proneural gene Neurogenin2 by Pax6, Development 130 (2003) 3269–3281.
[29] E.K. Schorry, M. Keddache, N. Lanphear, J.H. Rubinstein, S. Srodulski, D. Fletcher, R.I. Blough-Pfau, G.A. Grabowski, Genotype-phenotype correlations in Rubinstein–Taybi syndrome, Am. J. Med. Genet. A 146A (2008) 2512–2519.
[30] S.M. Sisodiya, S.L. Free, K.A. Williamson, T.N. Mitchell, C. Willis, J.M. Stevens, B.E. Kendall, S.D. Shorvon, I.M. Hanson, A.T. Moore, V. van Heyningen, PAX6 haploinsufficiency causes cerebral malformation and olfactory dysfunction in humans, Nat. Genet. 28 (2001) 214–216.
[31] S. Sukumar, S. Wang, K. Hoang, C.M. Vanchiere, K. England, R. Fick, B. Pagon, K.S. Reddy, Subtle overlapping deletions in the terminal region of chromosome 6q24.2-q26: three cases studied using FISH, Am. J. Med. Genet. 87 (1999) 17–22.
[32] B.H. Ticho, C. Hilchie-Schmidt, R.T. Egel, E.I. Traboulsi, R.J. Howarth, D. Robinson, Ocular findings in Gillespie-like syndrome: association with a new PAX6 mutation, Ophthalmic Genet. 27 (2006) 145–149.
[33] T. Tominaga, W. Meng, K. Togashi, H. Urano, A.S. Alberts, M. Tominaga, The Rho GTPase effector protein, mDia, inhibits the DNA binding ability of the transcription factor Pax6 and changes the pattern of neurite extension in cerebellar granule cells through its binding to Pax6, J. Biol. Chem. 277 (2002) 47686–47691.
[34] C.C. Ton, H. Hirvonen, H. Miwa, M.M. Weil, P. Monaghan, T. Jordan, V. van Heyningen, N.D. Hastie, H. Meijers-Heijboer, M. Drechsler, B. Royer-Pokora, F. Collins, A. Swaroop, L.C. Strong, G.F. Saunders, Positional cloning and characterization of a paired box- and homeobox-containing gene from the aniridia region, Cell 67 (1991) 1059–1074.
[35] I. Tzoulaki, I.M. White, I.M. Hanson, PAX6 mutations: genotype-phenotype correlations, BMC Genet. 6 (2005) 27.
[36] V. van Heyningen, K.A. Williamson, PAX6 in sensory development, Hum. Mol. Genet. 11 (2002) 1161–1167.
[37] J.H. Wen, Y.Y. Chen, S.J. Song, J. Ding, Y. Gao, Q.K. Hu, R.P. Feng, Y.Z. Liu, G.C. Ren, C.Y. Zhang, T.P. Hong, X. Gao, L.S. Li, Paired box 6 (PAX6) regulates glucose metabolism via proinsulin processing mediated by prohormone convertase 1/3 (PC1/3), Diabetologia 52 (2009) 504–513.
[38] H.E. Xu, M.A. Rould, W. Xu, J.A. Epstein, R.L. Maas, C.O. Pabo, Crystal structure of the human Pax6 paired domain-DNA complex reveals specific roles for the linker region and carboxy-terminal subdomain in DNA binding, Genes Dev. 13 (1999) 1263–1275.

Jpn J Ophthalmol 2009;53:7–11
DOI 10.1007/s10384-008-0619-6

CLINICAL INVESTIGATION

Central Corneal Thickness in Japanese Children

Akiko Hikoya[1], Miho Sato[1], Kinnichi Tsuzuki[2], Yuka Maruyama Koide[1], Ryo Asaoka[1], and Yoshihiro Hotta[1]

[1]Department of Ophthalmology, Hamamatsu University School of Medicine, Hamamatsu, Japan; [2]Department of Ophthalmology, Aichi Children's Health and Medical Center, Obu, Japan

Abstract

Purpose: To determine the central corneal thickness (CCT) in Japanese children and to investigate the changes in CCT with increasing age.

Methods: Pachymetry was performed on 338 eyes of 169 patients undergoing eye muscle surgery under general anesthesia, and the intraocular pressure (IOP) was measured on 312 eyes of 156 of those same patients. Patients with abnormalities other than refractive errors and strabismus were excluded. Patients were divided into four groups: group 1, ≤1 year of age; group 2, 2–4; group 3, 5–9; and group 4, 10–18 years of age. Analysis of variance (ANOVA) was performed to determine the significance of the changes in CCT.

Results: The average CCT of the right eye was 544.3 ± 36.9 μm. The CCT was thinner in group 1 than in groups 3 and 4 (ANOVA, $P = 0.02$). There was a positive but weak correlation between IOP and CCT (IOP = 6.253 + 0.014 × CCT; $r^2 = 0.047$, $P = 0.007$).

Conclusions: CCT reaches the adult thickness in Japanese children by age 5 years. The average CCT is thinner in Japanese children than in Caucasians but thicker than in African American children. **Jpn J Ophthalmol** 2009;53:7–11

Key Words: central corneal thickness, child, general anesthesia, intraocular pressure, ultrasound pachymeter

Introduction

Measuring central corneal thickness (CCT) has become increasingly important, particularly for the diagnosis and management of glaucoma. The Ocular Hypertension Treatment Study reported that subjects with ocular hypertension had greater CCT,[1] and subjects with smaller CCT had a higher risk of developing glaucoma.[2]

Goldmann applanation tonometer measurement is based on the assumption that CCT is 500 μm, a thickness obtained from measurements of cadaver eyes. Because a permanent thinning or flattening of the cornea induces lower intraocular pressure (IOP) after refractive surgery,[3,4] special attention has been paid to the variability of CCT in the healthy population and in patients with various eye diseases. To obtain an accurate IOP value, measurements with the Goldmann applanation tonometer should be corrected by the CCT value.[5] Thus, measuring CCT has become essential for determining true IOP for glaucoma management.

Children with congenital glaucoma also have significantly thinner CCT than healthy children.[6,7] However, aphakic[8,9] and pseudophakic[10] children with glaucoma have significantly thicker CCT than healthy children. These findings then raise the question of why up to 45% of aphakic children who have thicker than average CCT develop glaucoma.[11] Muir et al.[12] speculated that CCT increases after cataract surgery because of endothelial cell damage, or because increased IOP injures the endothelial cells. Thus, measuring CCT in children who are at high risk for glaucoma, such as children with aphakic or pseudophakic eyes, is important.

Received: January 25, 2008 / Accepted: September 26, 2008
Correspondence and reprint requests to: Miho Sato, Department of Ophthalmology, Hamamatsu University School of Medicine, 1-20-1 Handa-yama, Higashi-ku, Hamamatsu 431-3192, Japan
e-mail: mihosato@hama-med.ac.jp

Jpn J Ophthalmol
Vol 53: 7–11, 2009

Another important factor that influences the CCT is race or ethnicity. The CCT of African American adults is thinner than that of Caucasian adults,[2,13] and lower IOP in African Americans may delay the diagnosis of glaucoma and determination of an appropriate treatment target.[14] CCT in the Japanese population has been found to be thinner than in Chinese and Filipino populations.[15]

These racial differences are also found in the pediatric population. African American children have thinner CCT than do Caucasian[16] or Hispanic children.[17] A literature search on PubMed did not extract any CCT data regarding healthy Japanese children. Knowing the normal range of CCT of Japanese children is important for diagnosing and treating pediatric glaucoma.

Thus, the purpose of this study was to determine the CCT in Japanese children and to investigate the changes in CCT with increasing age. To accomplish this, we measured the CCT of 338 eyes of 169 children ≤18 years of age by ultrasound pachymetry under general anesthesia.

Subjects and Methods

All patients scheduled for strabismus surgery under general anesthesia were recruited from Hamamatsu University School of Medicine and Aichi Children's Health and Medical Center from December 2005 to August 2007. Patients with corneal disease, a history of intraocular surgery, glaucoma, cataract, or eyelid abnormalities were excluded. Patients known to have abnormally thin corneas such as those with Down syndrome[18] or with Marfan syndrome,[19] or abnormally thick corneas such as those with aniridia,[20] were also excluded.

This study was approved by the Institutional Review Board of the Hamamatsu University School of Medicine and Aichi Children's Health and Medical Center. Full explanation of the research, including the measurement procedures for CCT and IOP was given, and written informed consent was obtained from a parent or legal guardian of each of the patients.

For controls, we measured the CCT of eight healthy subjects aged 26 to 52 years under topical anesthesia.

CCT was measured between 9:00 and 16:00 in the operating room with an ultrasound pachymeter (SP-100 Handy, 1640 Hz; Tomey, Nagoya, Japan). Measurements started within 5 min of endotracheal intubation. All patients were sedated by inhalation or intravenously, and a muscle relaxant was given before insertion of the airway tube. Sevoflurane and nitrous oxide were used to maintain surgical anesthesia during the surgery. The patient's eyelid was held open manually, with special care taken not to press on the eye. One drop of topical anesthesia (4% oxybuprocaine) was administered, and the central cornea was defined as the center of the pupil. The pachymeter probe was placed perpendicularly on the center of the cornea, and the average of eight measurements was recorded as the CCT. Next, the IOP was measured with a Tono-Pen XL (Reichert, Depew, NY, USA). All measurements were performed first on the right eye and then on the left eye.

For statistical purposes, only the data from the right eye were used. The patients were divided into four groups: group 1, ≤1 year of age; group 2, 2–4; group 3, 5–9; and group 4, 10–18 years of age. Statistical analysis was performed using StatView version J-5.0 for Windows (SAS Institute, Cary, NC, USA). Analysis of variance (ANOVA) with a Bonferroni post hoc test was used to determine the significance of any differences among the age groups. Paired t tests were used for comparisons between eyes. Linear regression was used to determine the correlation between CCT and IOP. A P value of <0.05 was considered to be statistically significant.

Results

We measured the CCT of 338 eyes of 169 subjects (87 boys, 82 girls) with a mean age of 6.01 ± 3.87 years and an age range of 8 months to 18 years. The patient age distribution and the IOP and CCT measurements are summarized in Table 1.

The average CCT of the right eye was 544.3 ± 36.9 μm (range, 429–648 μm). The CCT distribution is shown in Fig. 1. The CCT was significantly different between age groups (ANOVA $P = 0.0198$); it was significantly thinner in group 1 than in groups 3 or 4 ($P = 0.0071$ and 0.0157, respectively, Bonferroni; Table 1). The average CCT in group 4 was 550.6 μm, which was not significantly different from the mean CCT of the eight healthy adult subjects (525–586 μm).

Table 1. Subjects' characteristics and measurement of CCT and IOP

	n (%)	CCT (μm)	IOP (mmHg)
All patients	169 (100)		
Age distribution (years)		(right eye)	(right eye)
0–1	14 (8)	522 ± 26.7	14.07 ± 2.89
2–4	50 (30)	538 ± 36.6 *	14.14 ± 2.55
5–9	77 (45)	550 ± 36.7 **	14.13 ± 2.13
10–18	28 (17)	550 ± 37.5	12.88 ± 2.45

Values are means ± SD.
CCT, central corneal thickness; IOP, intraocular pressure.
*$P = 0.0071$.
**$P = 0.0157$.

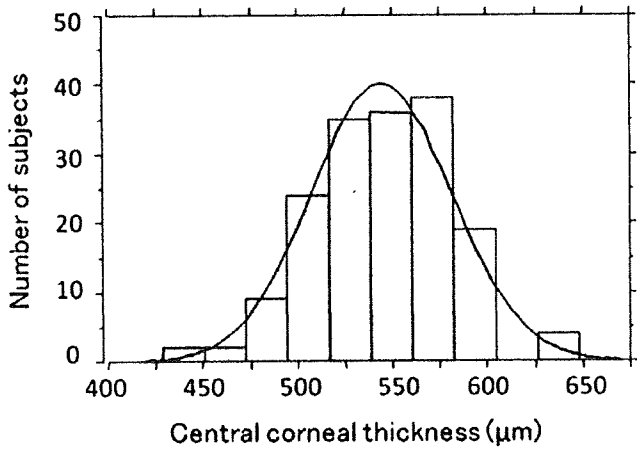

Figure 1. Distribution of central corneal thickness (CCT) in the right eye of children aged 0 to 18 years. CCT is normally distributed. The average CCT was 544.3 ± 36.9 μm.

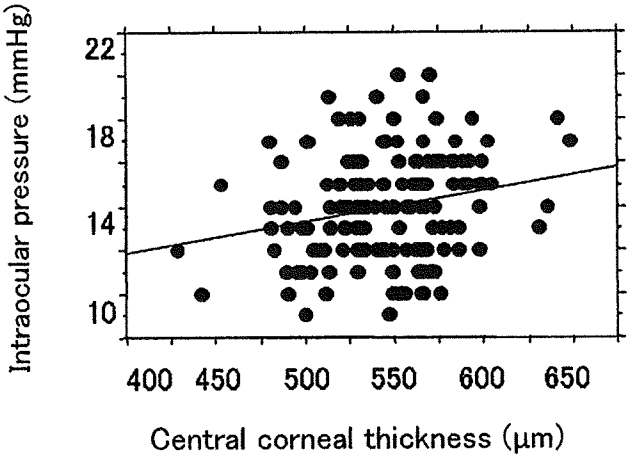

Figure 2. Relationship between CCT and intraocular pressure (IOP). There is a positive but weak correlation between CCT and IOP.

The mean CCT in our adults was comparable to the published average range for the adult Japanese population.[21,22]

The average IOP in the right eye was 13.9 ± 2.4 mmHg (range, 9.0–10.0 mmHg). The IOP did not differ significantly among the different age groups. IOP (y) and CCT (x) were positively correlated, but the correlation coefficient was low ($y = 6.253 + 0.014x$, $r^2 = 0.047$; $P = 0.007$; Fig. 2).

Discussion

Differences in CCT values measured with different instruments have been reported,[23–25] but the values obtained by ultrasound pachymetry and by noncontact optical low-coherence reflectometry are reported to be highly correlated.[26] Bovelle et al.[27] reported that the Topcon specular microscope gives significantly lower values than the ultrasound pachymeter. Suzuki et al.[21] compared CCT values obtained using Orbscan scanning-slit corneal topography/pachymetry, the Topcon SP-2000P, noncontact specular microscopy, and Tomey ultrasonic pachymetry in a Japanese population. The mean CCT was not significantly different between scanning-slit topography (546.9±35.4 μm) and ultrasonic pachymetry (548.1 ± 33.0 μm). However, contact specular microscopy gave a significantly smaller mean (525.3 ± 31.4 μm) than did the other two instruments.[21] Therefore, it is advisable not to compare CCT values obtained using different instruments.

Table 2. Comparison of CCT values of children by race

Race	Hussein[29] (μm)	Dai[17] (μm)	This study (μm)
Caucasians	551	563	
Hispanic	550	568	
Japanese			544
African Americans	532	523	

The SP100 ultrasonic pachymeter is compact and easy to use in the operating room. The measurements are accurate if the instrument is used appropriately. We took special care to place the probe on the center of the cornea because the cornea is thinnest at the center.[28,29]

In adults, CCT is negatively correlated with age in men,[30] or in both sexes.[31] In children, CCT is reported to decrease rapidly during the neonatal period,[32,33] and then to increase slowly and reach the adult level at 3[34] or 5 years of age.[29] Sawa[35] studied the Japanese population and found that the mean CCT of 1-month-old infants (534 ± 36 μm) is thicker than that of 3-month-old infants (508 ± 22 μm), but they found no difference between the 3-month-old infants and the 20- to 29-year-old adults (516 ± 17 μm). Muir et al.[36] suggested that CCT slowly increases in children up to the age of 5 and then decreases at around age 10–14 years. Hussein et al.[29] reported that CCT increases in children until age 9 years and then decreases between ages 10 and 14.[29] In our study, CCT was significantly less in group 1 than in groups 3 or 4, suggesting that adult CCT values are reached by 5 years of age.

Earlier studies have reported racial differences in CCT, not only in adults but also in children. Table 2 summarizes results from other countries for CCTs in pediatric populations from 0 to 18 years of age, measured with ultrasound pachymetry. We understand that it is not ideal to compare our data directly with those of previous reports, but as long as all the measurements were obtained with ultrasound pachymetry, it is reasonable to do so. Compared with the readings obtained from two different institutions,[17,29] the CCT of Japanese children still appears to be thicker than that of African American children and thinner than that of Caucasian or Hispanic children.

Studies focusing on the relationship between CCT and IOP have reported a significant correlation between IOP and CCT in children,[36] as in adults. Suzuki et al.[31] studied Japanese adults and found that IOP measured with the

Goldmann applanation tonometer was positively correlated with CCT. We found a positive correlation between CCT and IOP measured by Tono-Pen in children, but the correlation coefficient was low.

The Tono-Pen is generally used in children whose IOP is neither very high (>21 mmHg) nor very low (<9 mmHg).[37] IOPs obtained with Tono-Pen are significantly correlated with those obtained using the Goldmann tonotmeter.[38,39] IOPs measured with the Goldmann tonometer, the noncontact tonometer, and the Tono-Pen are known to be influenced by CCT, but IOPs measured by Tono-Pen are less affected by CCT than the other tonometers.[40,41]

We are aware that measured IOP differs significantly with the type and state of anesthesia; for example, succinylcholine can increase IOP, whereas halothane can reduce it.[42] In addition, IOP in the human infant depends strongly on the level of relaxation.[42]

In conclusion, the CCT of Japanese children increases up to age 5 years, when it does not differ significantly from that of adults. The CCT of Japanese children is thinner than that of Caucasian children but thicker than that of African American children. Knowing the average CCT value in the Japanese pediatric population will be useful when caring for not only congenital anomalies involving the cornea but also pediatric glaucoma.

References

1. Brandt JD, Beiser JA, Kass MA, Gordon MO. Central corneal thickness in the Ocular Hypertension Treatment Study (OHTS). Ophthalmology 2001;108:1779–1788.
2. Gordon MO, Beiser JA, Brandt JD, et al. The Ocular Hypertension Treatment Study: baseline factors that predict the onset of primary open-angle glaucoma. Arch Ophthalmol 2002;120:714–720; discussion 829–830.
3. Chatterjee A, Shah S, Bessant DA, et al. Reduction in intraocular pressure after excimer laser photorefractive keratectomy. Correlation with pretreatment myopia. Ophthalmology 1997;104:355–359.
4. Mardelli PG, Piebenga LW, Whitacre MM, Siegmund KD. The effect of excimer laser photorefractive keratectomy on intraocular pressure measurements using the Goldmann applanation tonometer. Ophthalmology 1997;104:945–948; discussion 9.
5. Ehlers N, Bramsen T, Sperling S. Applanation tonometry and central corneal thickness. Acta Ophthalmol (Copenh) 1975;53:34–43.
6. Henriques MJ, Vessani RM, Reis FA, et al. Corneal thickness in congenital glaucoma. J Glaucoma 2004;13:185–188.
7. Wygnanski-Jaffe T, Barequet IS. Central corneal thickness in congenital glaucoma. Cornea 2006;25:923–925.
8. Simon JW, O'Malley MR, Gandham SB, et al. Central corneal thickness and glaucoma in aphakic and pseudophakic children. J AAPOS 2005;9:326–329.
9. Tai TY, Mills MD, Beck AD, et al. Central corneal thickness and corneal diameter in patients with childhood glaucoma. J Glaucoma 2006;15:524–528.
10. Simsek T, Mutluay AH, Elgin U, et al. Glaucoma and increased central corneal thickness in aphakic and pseudophakic patients after congenital cataract surgery. Br J Ophthalmol 2006;90:1103–1106.
11. Kirwan C, O'Keefe M. Paediatric aphakic glaucoma. Acta Ophthalmol Scand 2006;84:734–739.
12. Muir KW, Duncan L, Enyedi LB, et al. Central corneal thickness: congenital cataracts and aphakia. Am J Ophthalmol 2007;144:502–506.
13. La Rosa FA, Gross RL, Orengo-Nania S. Central corneal thickness of Caucasians and African Americans in glaucomatous and nonglaucomatous populations. Arch Ophthalmol 2001;119:23–27.
14. Shimmyo M, Ross AJ, Moy A, Mostafavi R. Intraocular pressure, Goldmann applanation tension, corneal thickness, and corneal curvature in Caucasians, Asians, Hispanics, and African Americans. Am J Ophthalmol 2003;136:603–613.
15. Aghaian E, Choe JE, Lin S, Stamper RL. Central corneal thickness of Caucasians, Chinese, Hispanics, Filipinos, African Americans, and Japanese in a glaucoma clinic. Ophthalmology 2004;111:2211–2219.
16. Muir KW, Duncan L, Enyedi LB, Freedman SF. Central corneal thickness in children: Racial differences (black vs. white) and correlation with measured intraocular pressure. J Glaucoma 2006;15:520–523.
17. Dai E, Gunderson CA. Pediatric central corneal thickness variation among major ethnic populations. J AAPOS 2006;10:22–25.
18. Evereklioglu C, Yilmaz K, Bekir NA. Decreased central corneal thickness in children with Down syndrome. J Pediatr Ophthalmol Strabismus 2002;39:274–277.
19. Sultan G, Baudouin C, Auzerie O, et al. Cornea in Marfan disease: Orbscan and in vivo confocal microscopy analysis. Invest Ophthalmol Vis Sci 2002;43:1757–1764.
20. Brandt JD, Casuso LA, Budenz DL. Markedly increased central corneal thickness: an unrecognized finding in congenital aniridia. Am J Ophthalmol 2004;137:348–350.
21. Suzuki S, Oshika T, Oki K, et al. Corneal thickness measurements: scanning-slit corneal topography and noncontact specular microscopy versus ultrasonic pachymetry. J Cataract Refract Surg 2003;29:1313–1318.
22. Wu LL, Suzuki Y, Ideta R, Araie M. Central corneal thickness of normal tension glaucoma patients in Japan. Jpn J Ophthalmol 2000;44:643–647.
23. Thomas J, Wang J, Rollins AM, Sturm J. Comparison of corneal thickness measured with optical coherence tomography, ultrasonic pachymetry, and a scanning slit method. J Refract Surg 2006;22:671–678.
24. Kim HY, Budenz DL, Lee PS, et al. Comparison of central corneal thickness using anterior segment optical coherence tomography vs ultrasound pachymetry. Am J Ophthalmol 2008;145:228–232.
25. Mishima S. Corneal thickness. Surv Ophthalmol 1968;13:57–96.
26. Airiani S, Trokel SL, Lee SM, Braunstein RE. Evaluating central corneal thickness measurements with noncontact optical low-coherence reflectometry and contact ultrasound pachymetry. Am J Ophthalmol 2006;142:164–165.
27. Bovelle R, Kaufman SC, Thompson HW, Hamano H. Corneal thickness measurements with the Topcon SP-2000P specular microscope and an ultrasound pachymeter. Arch Ophthalmol 1999;117:868–870.
28. Remon L, Cristobal JA, Castillo J, et al. Central and peripheral corneal thickness in full-term newborns by ultrasonic pachymetry. Invest Ophthalmol Vis Sci 1992;33:3080–3083.
29. Hussein MA, Paysse EA, Bell NP, et al. Corneal thickness in children. Am J Ophthalmol 2004;138:744–748.
30. Nomura H, Ando F, Niino N, et al. The relationship between age and intraocular pressure in a Japanese population: the influence of central corneal thickness. Curr Eye Res 2002;24:81–85.
31. Suzuki S, Suzuki Y, Iwase A, Araie M. Corneal thickness in an ophthalmologically normal Japanese population. Ophthalmology 2005;112:1327–1336.
32. Autzen T, Bjornstrom L. Central corneal thickness in full-term newborns. Acta Ophthalmol (Copenh) 1989;67:719–720.
33. Autzen T, Bjornstrom L. Central corneal thickness in premature babies. Acta Ophthalmol (Copenh) 1991;69:251–252.
34. Ehlers N, Sorensen T, Bramsen T, Poulsen EH. Central corneal thickness in newborns and children. Acta Ophthalmol (Copenh) 1976;54:285–290.

35. Sawa M. Measurement of corneal thickness. Jap Rev Clin Ophthalmol (Ganka Rinsho Iho) 1986;80:177–184.
36. Muir KW, Jin J, Freedman SF. Central corneal thickness and its relationship to intraocular pressure in children. Ophthalmology 2004;111:2220–2223.
37. Kao SF, Lichter PR, Bergstrom TJ, et al. Clinical comparison of the Oculab Tono-Pen to the Goldmann applanation tonometer. Ophthalmology 1987;94:1541–1544.
38. Bordon AF, Katsumi O, Hirose T. Tonometry in pediatric patients: a comparative study among Tono-pen, Perkins, and Schiotz tonometers. J Pediatr Ophthalmol Strabismus 1995;32:373–377.
39. Dohadwala AA, Munger R, Damji KF. Positive correlation between Tono-Pen intraocular pressure and central corneal thickness. Ophthalmology 1998;105:1849–1854.
40. Bhan A, Browning AC, Shah S, et al. Effect of corneal thickness on intraocular pressure measurements with the pneumotonometer, Goldmann applanation tonometer, and Tono-Pen. Invest Ophthalmol Vis Sci 2002;43:1389–1392.
41. Yildirim N, Sahin A, Basmak H, Bal C. Effect of central corneal thickness and radius of the corneal curvature on intraocular pressure measured with the Tono-Pen and noncontact tonometer in healthy schoolchildren. J Pediatr Ophthalmol Strabismus 2007;44: 216–222.
42. Dominguez A, Banos S, Alvarez G, et al. Intraocular pressure measurement in infants under general anesthesia. Am J Ophthalmol 1974;78:110–116.

わかりやすい
臨床講座

小児白内障の治療

黒 坂 大次郎

〔要 約〕

小児期の白内障治療を成功させるためには，適切に手術適応を判断し，術後管理を行うことが重要である。手術適応は，白内障の混濁程度，弱視の有無を見極め，患児の年齢に応じた手術目的（例えば学童以前であれば弱視予防）にそって判断する。また，乳幼児期の眼内レンズ挿入は，長所も大きいが，短所もあること，特別な手術手技や管理が必要なことを理解した上で慎重に行うべきである。

はじめに

成人の白内障の治療は，超音波乳化吸引術（PEA）による水晶体内容の除去と眼内レンズ挿入という術式がほぼ確立し，特殊な場合を除き安定した成績を得られる時代となった。多くの特殊なケースでも治療の基本方針は変わらない。だが，小児の場合には，確かに技術的な面は一部を除きほぼ成人のものと共通であるが，状況が異なる。例え成人と同じことを行ったとしても組織の反応，視機能予後，術後合併症などは異なり術後の経過観察のポイントも異なる。成人の白内障手術で確立した技術を最大限に応用しながら，小児の特殊性を踏まえた対応を取ることが，治療の最大のポイントである。

Ⅰ．白内障の診断と手術適応

1．白内障の診断

白内障の診断は，基本的に細隙灯顕微鏡で行う。乳幼児であれば，抑制・睡眠下の手持ち細隙灯顕微鏡検査が必要になる。できるだけ散瞳させ，よく観察することが重要である。瞳孔領との関係を明らかにしたい場合や，一部特殊な水晶体異常（後部円錐水晶体）などでは，スキアスコピーの際の反帰光の動きを観察するとわかりやすい。混濁の部位，程度をよく観察する。また，小眼球・小角膜・先天虹彩欠損の合併，散瞳不良などは，眼の未熟性を示唆するので注意して診察する。

2．全身疾患・他の眼疾患の検索

白内障がある場合は，手術治療や経過観察（健眼遮蔽など）が必要となるが，治療方針決定の大まかな手順を表1から3に示す。まずは，全身疾患・他の眼疾患を伴っているかを検討する（表1）。白内障は，ダウン症候群などの全身疾患に合併することがあり，小児科的な検索が必要で，例えば，先天性心疾患を伴っている場合などは全身の治療が優先される。緑内障，角膜，網膜などの眼疾患があると，それらの視機能予後を加味した上での総合的な判断が必要になる。基本的には，基礎疾患の管理が優先される。

表1 治療方針決定のステップ1（基礎疾患の有無）

- 全身疾患を伴っているか（小児科的検索）
- 他の眼合併症を伴っているか
  伴っている場合は，基礎疾患の治療を優先させる

黒坂大次郎：岩手医科大学眼科

3. 視性刺激遮断弱視

重篤な全身疾患・眼合併症が無い場合には，次に白内障を手術すべきかどうかの判断を行う。このステップは弱視の有無・患児の年齢によって対応が異なるが，まずは弱視の有無から診断する（表2）。生後2-3週から学童期以前（特に乳幼児期）は，視力を獲得する時期にあたり，この時期に強い白内障が一定期間以上存在すると視性刺激遮断弱視になっている危険性がある。この弱視は，強固になると治療に抵抗性のため，白内障手術をしても視機能の獲得・回復は望めなく，手術適応は少ない。従って，強固な視性刺激遮断弱視が存在するかどうかの判断が重要になる。白内障の混濁程度と発症時期，斜視などの眼所見の有無から判断する。

視性刺激遮断弱視を生じるためにはある程度以上の混濁が必要で，両眼例で左右差が無い場合は，散瞳しても眼底が透見できない程度の混濁が必要である（図1）。片眼性例や左右差のある両眼例では，混濁の程度が軽くても弱視になりやすい。それゆえ判断に迷う場合が多いが，Wrightら[1]の報告を参考に弱視になるリスクを判断する（表4）。次に上記のような混濁がある場合に，強固な視性刺激遮断弱視がすでに存在しているかどうかの判断を行う。両眼性で眼振が出現し一定期間以上を経過している

表2　治療方針決定のステップ2
（視性刺激遮断弱視を疑う所見）

- ●両眼性
  - 混濁程度
    - 混濁で眼底が透見できないもの
    - 混濁の左右差があるもの
  - 随伴所見：眼振
- ●片眼性
  - 混濁程度
    - 混濁が中心部で濃い（表4参照）
  - 随伴所見：斜視

表3　治療方針決定のステップ3（手術適応と年齢）

- ●学童期以前
  - 弱視となるまたは悪化させる危険性が高い場合
    - 生後3週以内で混濁の強い片眼例
    - 生後4-6ヶ月以内で眼底が透見できない両眼例
    - 両眼例で眼振が出現した直後
- ●学童期以後
  - 日常・学校生活に支障を来す場合

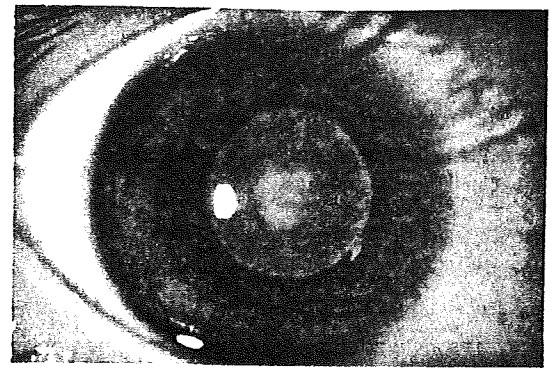

図1　層間白内障
左右差が無く眼振が認められない場合は，手術は学童期以降でよい。

表4　手術が必要になる白内障の形態学的特徴

手　術	経過観察
＞4 mm（混濁径）	＜3 mm（混濁径）
中央部の混濁	周辺部の混濁
後極部よりの混濁	前極部よりの混濁
密な混濁	点状混濁（一部が透明）

（文献1より改変して引用）

か，片眼性で斜視が出現している場合に視性刺激遮断弱視が強固になっていると判断する。

4. 手術適応と年齢

視性刺激遮断弱視が強固になっていない場合に手術を検討する（表3）。手術適応を考える上で重要なのは，患児の年齢である。学童期以前（特に乳幼児期）は，視力を獲得する時期にあたり，この獲得に白内障が障害となる場合にのみ弱視予防目的で手術を行う。それ以外は，経過観察が基本であり，学童期になってから手術を検討する（成人では視力が1.0であっても混濁を除去し視機能の向上が望めるのであれば手術を行うが，小児では，年齢によっては弱視に陥らない混濁は除去すべきでない）。ただし経過観察中に，白内障が進行し，眼振など視性刺激遮断弱視を疑わせる所見が認められたらば，すぐに手術を行う必要がある。学童期以後は，すでに視力を獲得している時期にあたり，成人の場合と同じようにすでに獲得された視力が白内障により低下している場合，これを回復させるために手術を行う。ただ，老視になって調節力が減弱している世代の手術と違って，調節力のある世代での手術になるので，調節力が失われる欠点も考慮のうえ，手術が患児の日常・学校生活にとってプラスになるか検討し手術適応を決める。